

METEOROLOGICAL INFLUENCES ON LORAN-C PROPAGATION  
OVER SEA AND LAND IN MEDITERRANEAN SEA CHAIN

Zoran M. Marković

Federal Bureau of Measures and Precious Metals  
Mike Alasa 14, 11000 Belgrade, Yugoslavia

ABSTRACT

Loran-C phase variations of signal from the Master of the Mediterranean Sea chain at Sellia Marina were measured simultaneously at three receiving sites, located on sea, coast and land. The effect of terrain over which the signal is propagated is considered together with the influence of weather parameters on the phase variations at the transmitter, along the signal paths and at the receiving sites. Based on an analysis of these data, correlations among these variations are examined, and correction is introduced to the measured results, in order to improve precision of mutual and international comparisons via Loran-C.

INTRODUCTION

Eleven collaborating laboratories which contribute data on atomic time - TAI use Mediterranean Sea Loran-C chain for their international comparisons, five of which receive the signals from Master station, 7990-M [1].

International comparisons of the cesium clock in Federal Bureau of Measures and Precious Metals, UTC(YUZM), for twelve years now, have been carried out via Loran-C, Master at Sellia Marina, and by clock transportation [2]. Variations of phase of a received Loran-C signal in Belgrade have been observed as seasonal, as well as diurnal [3]. These variations have also been studied elsewhere in the world [4] - [7], but our intention was to study them for our particular propagation path.

An experiment aimed at analysis of Loran-C time of arrival - TOA variations on sea and land was realized in July 1987.

Using three Loran-C receivers, times of arrivals of the signals from the Master of the Mediterranean Sea chain were measured simultaneously on sea, coast and land, in relation to the times of atomic clocks on the island, in Split and in Belgrade, respectively. Together with TOA measurements, temperature of air at receiving antenna sites was also measured. In order to analyze correlations between time of arrival variations and weather parameters, meteorological data were obtained from meteorological stations along the propagation paths.

#### ANALYSIS OF PHASE VARIATIONS AT DIFFERENT RECEIVING SITES

Geometry of receiving sites during the experiment on sea, coast and land in relation to Master at Sellia Marina is shown in Figure 1, together with geographical configuration of the paths over which Loran-C ground wave signal is propagated. The layout of meteorological stations located close along the propagation paths, which supplied information on air temperature, humidity and pressure, are also shown in Figure 1.

Elevation profiles for two propagation paths are shown in Figure 2, since the path towards the island coincides for the most part with the path of receiving site located in Split. Elevations of meteorological stations are shown on these profiles, but it should be noted that air pressures measured in them were reduced to sea level for the purpose of calculations and analyses. In order to examine meteorological influences, the paths were divided into segments, presuming that characteristics of propagation medium within each segment were nearly the same from meteorological point of view.

The measurement system used in Belgrade is described in reference [3], and it was almost the same in other two sites. Characteristics of atomic clocks were determined in the beginning and at the end of the experiment by clock transportation, so that the rate of atomic clocks during the experiment was determined and removed from the data. Measurements were carried out every second with resolution of 20 ps. Results of measurement were filtered by means of a recursive discrete filter which approximates a special case of Wiener filter,

$$x_i = \frac{1}{\tau + 1} (x_i + \tau x_{i-1}) \quad (1)$$

where  $\tau$  amounts to 14 400. By filtering data, time of arrival variations were reduced by about 3.5 times.

Figure 3 presents time of arrival variations following filtering for receiving sites on sea, coast and land with phase

variations being larger in signals propagated over land and traversing a mountain range. A correlation between these variations is observed, resulting from phase changes in the transmitter and following propagation through the common part of the medium. Phase variations which are neither recorded at the same time, nor are they of equal intensity at all the three sites, appear mainly due to changes in the medium in the vicinity of the receiving antenna.

#### METEOROLOGICAL INFLUENCES ON GROUND WAVE PROPAGATION

Total phase lag  $\phi$ , of propagated ground wave of Loran-C signal can be expressed as [5]

$$\phi = \frac{\omega}{c} n_a^\alpha + d_c \quad (2)$$

where  $n$  is the surface refractive index,  $d$  is the distance between the transmitter and the receiver in meters,  $\omega/c = 3.3355693$  ns/m, and  $\phi_c$  is the secondary phase correction, which can be determined approximately from [8]

$$\phi_c = (n_a^\alpha \omega/c)^{1/3} \tau_0^{2/3} (d/a) \quad (3)$$

where  $a$  is the radius of the Earth,  $\tau_0$  is derived from the boundary condition at the surface of the ground, and  $\alpha$  is associated with the slope of the profile of refractive index with altitude. Over average land  $\tau_0$  is of the order of 0.89.

Phase of the primary wave depends directly on  $n$ . But the phase of the secondary factor depends on  $n$ , gradient of  $n$  through factor  $\alpha$ , and the ground surface impedance which enters into  $\tau_0$ . Parameter  $\alpha$  is a function of surface refractive index and its gradient with respect to altitude  $Z$ , or lapse rate, and is given by

$$\alpha = 1 + \frac{a}{n} \frac{dn}{dz} \quad (4)$$

Weather parameters, such as temperature, pressure and humidity, influence the behavior of atmospheric refractive index [9] in a complex way, but the following simplified formula relating the refractive index with these various parameters has been found to be useful in practical work in radiometeorological studies,

$$(n - 1) 10^6 = N = \frac{77.6}{T} (P + \frac{4810e}{T}) \quad (5)$$

where  $N$  is refractivity,  $T$  is temperature in K,  $P$  is atmospheric pressure in mb, and  $e$  is partial water vapour pressure in mb. The second term of eqn. (5) contains humidity term  $e$ , and it is therefore called the wet term. The first term is known as the dry term.

Comparative analysis of TOA variations and refractivity ( $N_{\text{total}}$ ) changes for the three receiving sites did not offer a satisfactory correlation. This can be explained by the fact that lapse rate is practically constant in summer, as well as that wet term amounted to 20 % of the refractivity ( $N_{\text{total}}$ ) all the time in the area observed by the experiment.

A significant (negative) correlation between TOA variations and the changes of dry term of refractivity is shown in references [5] and [6]. Variations of TOA at different receiving sites with integrated dry term,  $N_{\text{dry}}$ , data for each particular path, are plotted in Figure 4. Integrated dry term,  $N_{\text{dry}}$ , data were obtained as a weighted mean of  $N_{\text{dry}}$  from all segments of a particular path according to length of the segments, as they are shown in Figure 2. High degree of (negative) correlation is obvious for all the three receiving sites, i.e. on sea, coast and land.

However, it is not always possible to obtain meteorological data for calculation of integrated dry term from a large number of meteorological stations along propagation path, especially not with the frequency which would be necessary. In Europe, signal path frequently crosses over several states, making this problem even more serious. In a situation where only dry term is important, as shown in references [5] and [7], secondary phase factor increases (decreases) with the increase (decrease) of the values of  $\alpha$ . This implies that when temperature increases (decreases), both  $\alpha$  and TOA (time of arrival) increase (decrease), which may be interpreted as high positive correlation between temperature and TOA variations.

Instead of further examination of the correlation between TOA variations and the changes of integrated air temperature which could be obtained as the weighted mean from temperatures associated with corresponding segments along the path, it was decided to examine the correlation between TOA variations and air temperature changes at the receiving site. Figure 5 presents TOA variations together with air temperature changes at the receiving site for the three receiving sites on sea, coast and land. The figure clearly shows high degree of correlation between the presented temperature changes and the time of arrival variations for different receiving sites.

A common presentation of air temperature and corresponding time of arrival for the receiving sites on sea, coast and land is given in Figure 6. Each datum is a couple of measured values at the moment results were recorded. The straight line which is the best approximation of the dependence between time of arrival variations and air temperature changes has been

determined by the method of linear least square fit, and it is presented in this Figure. Time of arrival variation of Loran-C signal, due to air temperature change (coefficient equal to the slope of the straight line), amounted to  $A_1 = 3.3 \text{ ns}/^\circ\text{C}$  for the receiving site on sea,  $A_2 = 3.1 \text{ ns}/^\circ\text{C}$  for the receiving site on coast, and  $A_3 = 3.1 \text{ ns}/^\circ\text{C}$  for the receiving site on land. In June 1986 the coefficient was  $A = 2.8 \text{ ns}/^\circ\text{C}$  for the same receiving site on land, in Belgrade. During the winter this coefficient can be as high as  $A = 78 \text{ ns}/^\circ\text{C}$ , as it was in November 1985 for the receiving site in Belgrade [10].

Time of arrival values  $t$  (ns), presented in Figure 3, obtained after filetring, were corrected by application of linear dependence shown in Figure 6, by means of the following equation

$$t_k = t - AT \quad (6)$$

where  $t_k$  is corrected time of arrival in ns,  $A$  is the coefficient (slope of straight lines from Fig. 6) in  $\text{ns}/^\circ\text{C}$ , and  $T$  is air temperature in  $^\circ\text{C}$ .

Figure 7 shows Loran-C time of arrival variations after correction for the value of corresponding air temperature has been introduced, for the receiving sites on sea, coast and land. After correction, the effective value of variations was reduced by about 2 times for all three receiving sites. Even after correction, phase variations are larger in signals propagated over land than in those propagated over sea. Time of arrival variation after correction was in Split 4.9 ns ( $1\sigma$ ), and in Belgrade 6.0 ns ( $1\sigma$ ), meaning that after correction uncertainty in comparison between Belgrade and Split was 7.7 ns ( $1\sigma$ ). Minimum time of arrival variations were during the day, between 11 a.m. and 3 p.m., when total variations of the corrected phase was around 10 ns. The possibility of comparison of atomic clocks in Belgrade and Split by Loran-C is actually the difference of times of arrival of these two cities. Total variation of the difference of corrected times of arrival is below 50 ns.

#### CONCLUSION

Loran-C phase variations of signal from the Master of the Mediterranean Sea chain measured at receiving sites on sea, coast and land are significantly correlated with integrated dry term of refractivity as well as with air temperature at the receiving site. By presenting time of arrival as a linear function of air temperature, applying the linear least square fit method, it is possible to introduce a correction on measured results,

which enables reduction of time of arrival variations by factor 2 for all three receiving sites. It is shown that even a simple correction based on a single influence quantity, considerably improves precision of mutual and international comparisons via Loran-C.

#### ACKNOWLEDGEMENT

The author wishes to acknowledge Prof.Dr. Dragan Stanković and Mr. Vlado Mamula for their contributions in collecting and analysis of the data.

#### REFERENCES

1. BIPM, BIH Annual Report for 1987.
2. Z.M. Marković and S. Hajduković, "The time and frequency comparisons via Loran-C and National TV network in Yugoslavia", in Proc. 16th Annual PTTI Meeting, pp. 419-426, November 1984.
3. Z.M. Marković, "Long-term stability of Yugoslav primary time and frequency standard", Master's thesis, University of Belgrade, 1986.
4. G.M.R. Winkler, "Path delay, its variations, and some implications for the field use of precise frequency standards", Proc. IEEE, Vol. 60, No. 5, pp. 522-529, May 1972.
5. R.H. Doherty and J.R. Johler, "Meteorological influences on Loran-C ground wave propagation", J. Atmospheric and Terrestrial Physics, Vol. 37, pp. 1117-1124, 1975.
6. W.N. Dean, "Diurnal variations in Loran-C groundwave propagation", in Proc. 9th Annual PTTI Meeting, pp. 297-316, March 1978.
7. S.N. Samaddar, "Weather effect on Loran-C propagation", Navigation: J. Inst. of Navigation, Vo. 27, No.1, pp. 39-53, 1980.
8. J.R. Johler, W.J. Kellar, and L.C. Walters, "Phase of the low radiofrequency ground wave", NBS Circular 573, June 1956.
9. B.R. Bean and E.S. Dutton, "Radio Meteorology", NBS Monograph 92, March 1966.
10. Z.M. Marković, "Air temperature Loran-C time of arrival correlationsrelationships", in press.



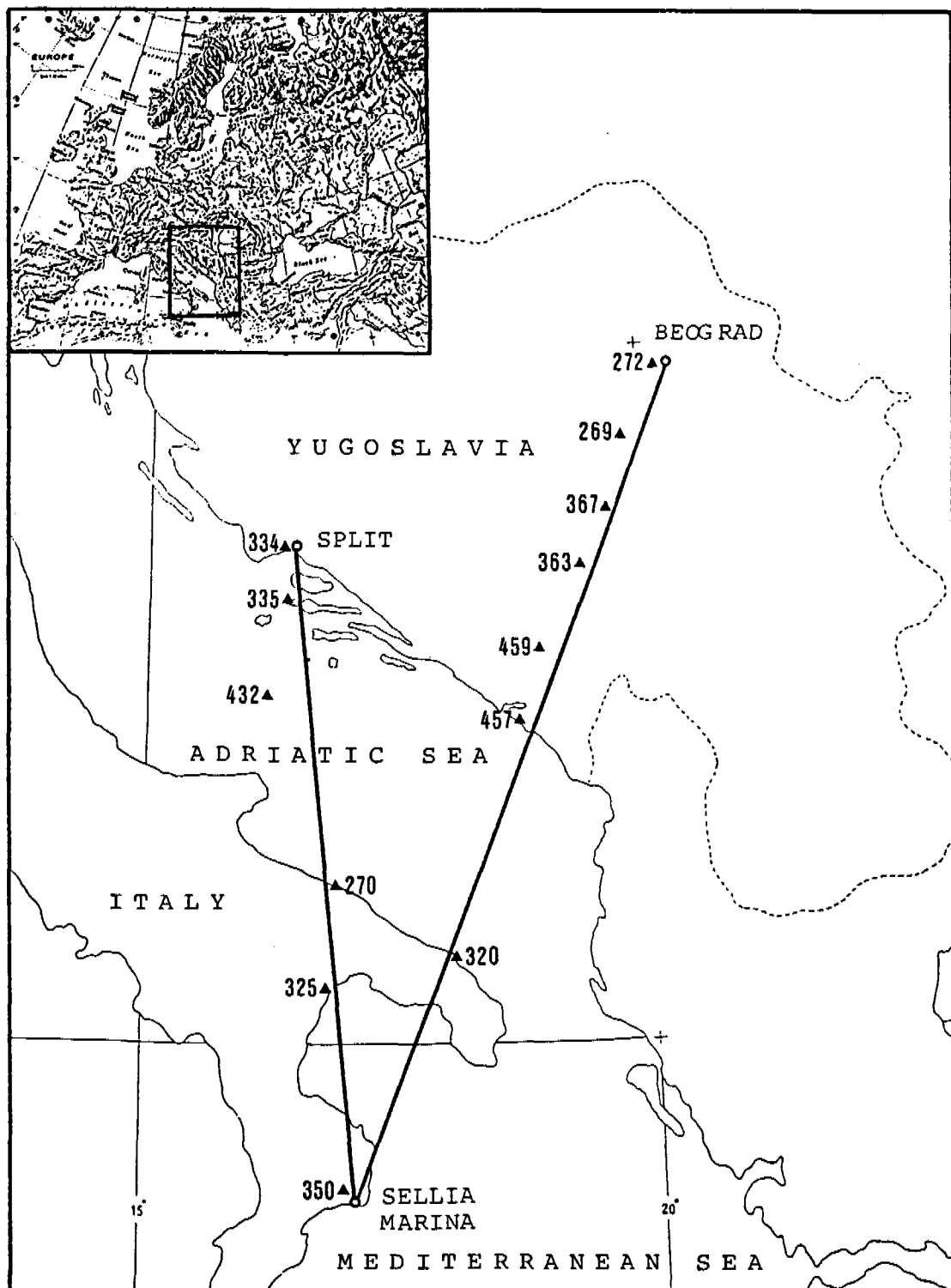


Figure 1. Geometry of receiving sites in relation to Master at Sellia Marina and meteorological stations designated by codes

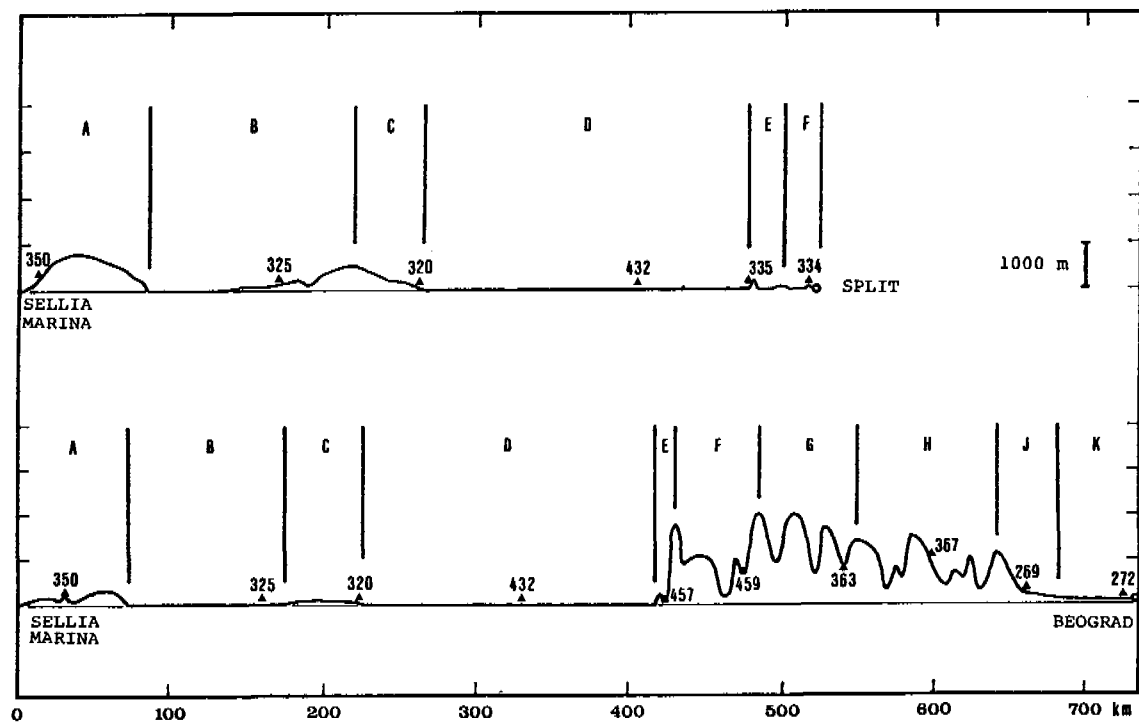


Figure 2. Elevation profiles of paths over which Loran-C signal is propagated and meteorological stations with corresponding segments of the paths

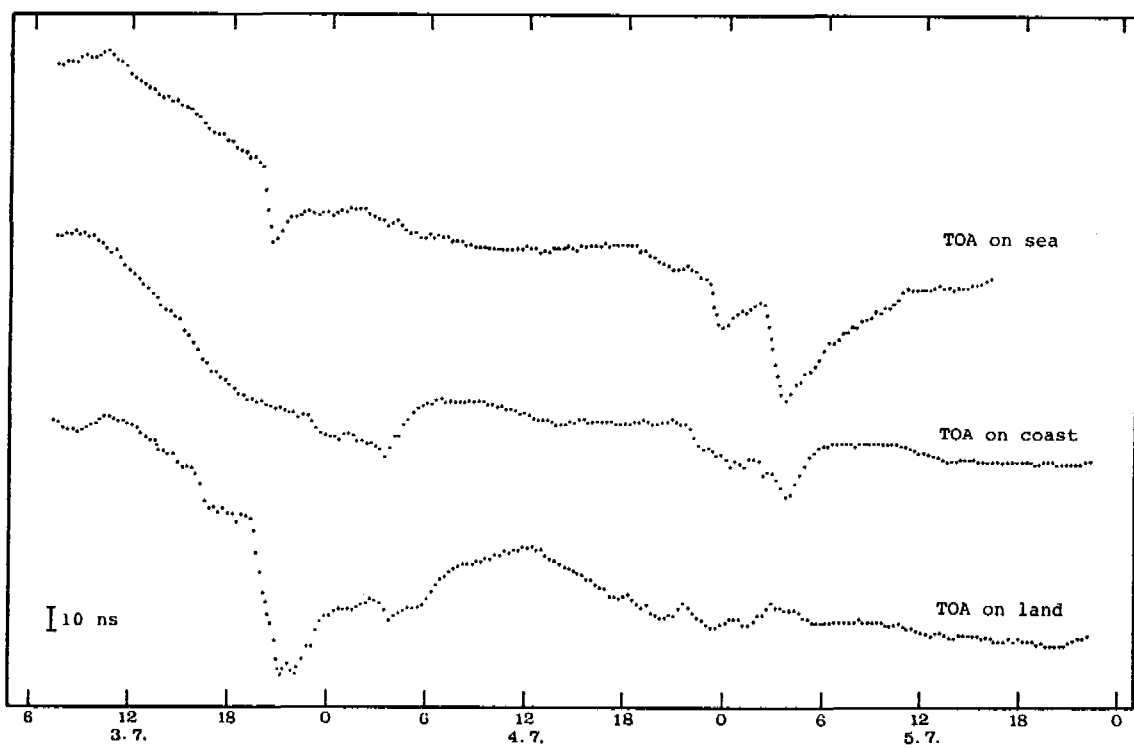


Figure 3. Loran-C time of arrival variations at different receiving sites

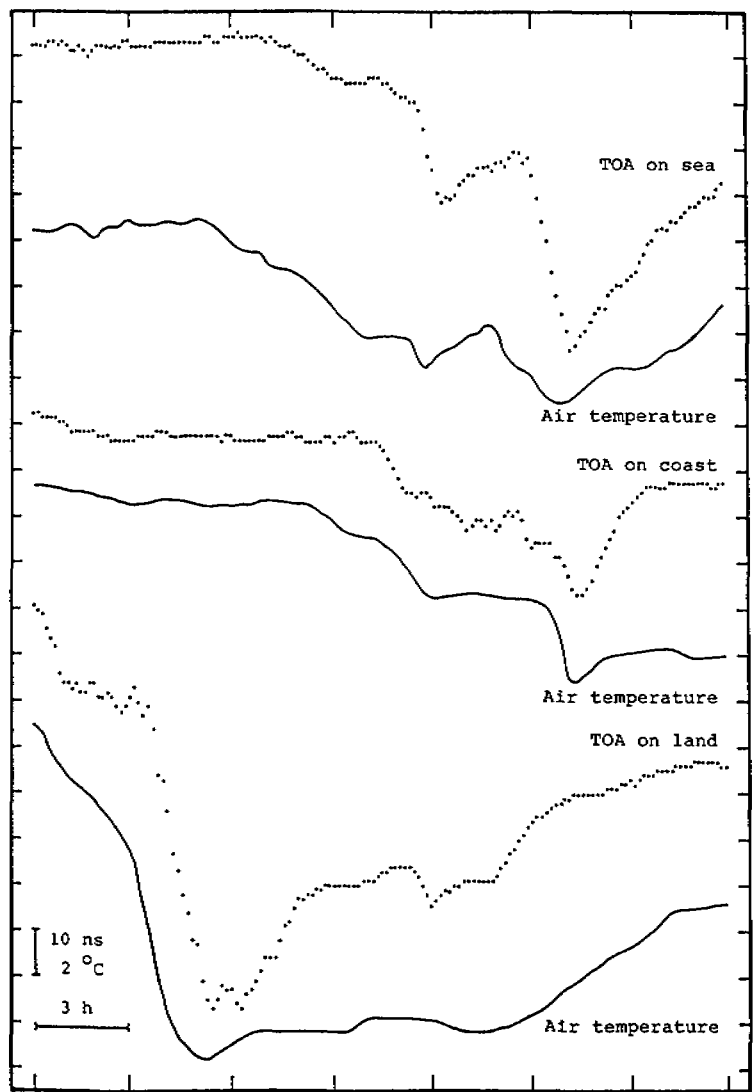


Figure 5. Loran-C time of arrival variations with air temperature changes at different receiving sites

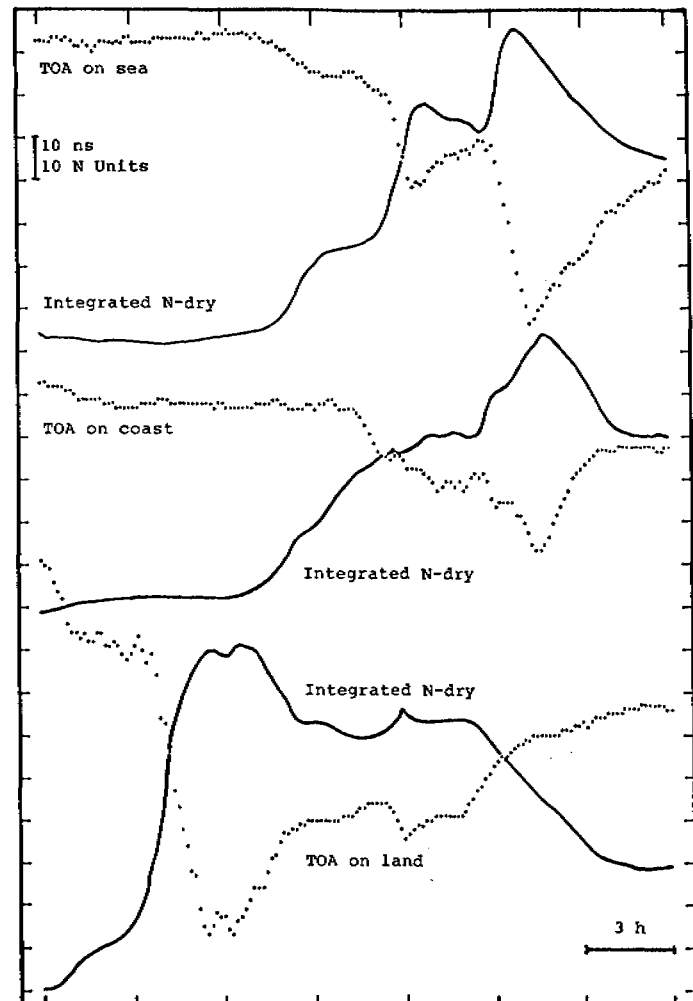


Figure 4. Loran-C time of arrival variations at different receiving sites with integrated N-dry changes along the corresponding paths

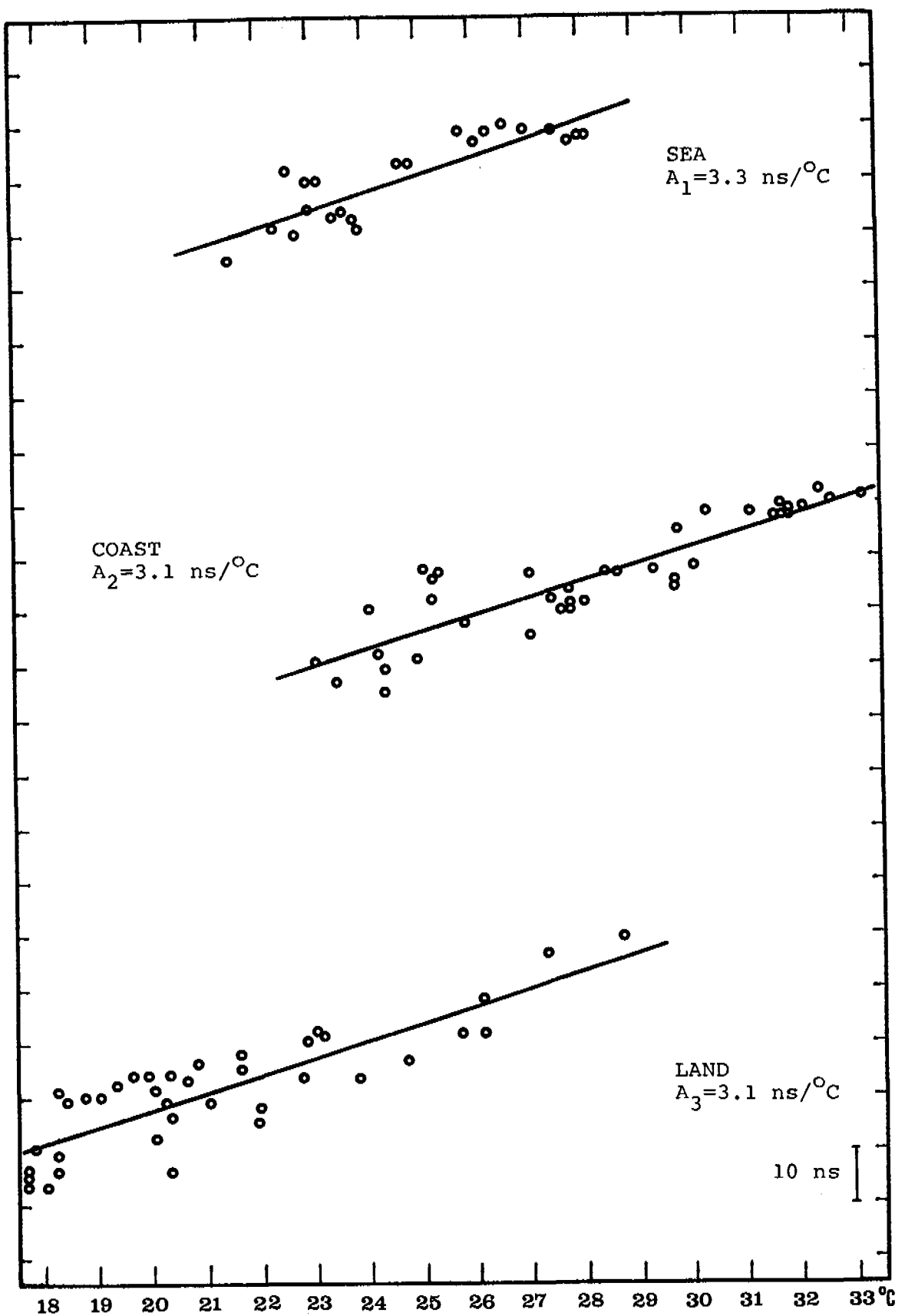


Figure 6. Common presentation of air temperature and time of arrival at different receiving sites

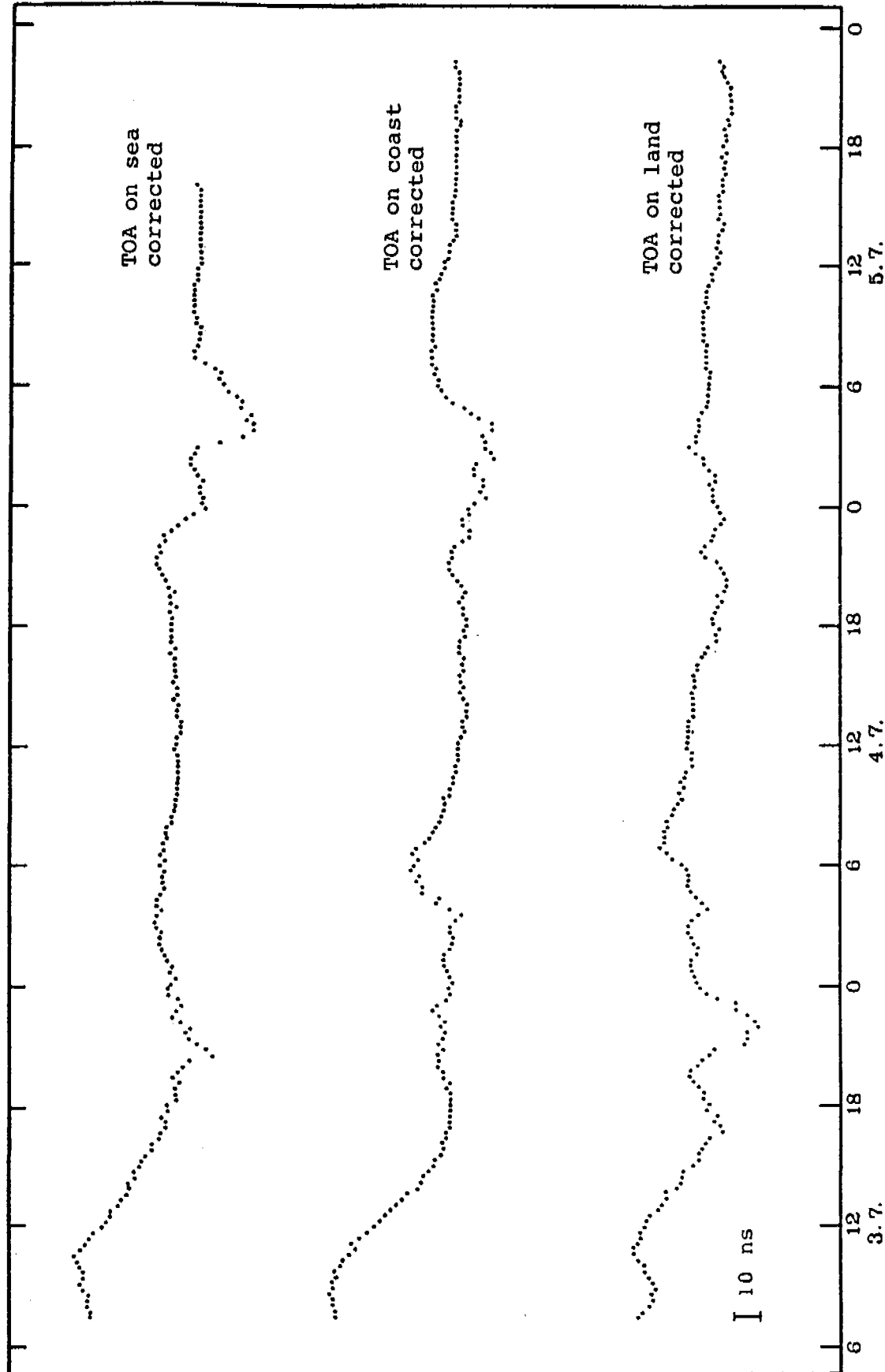


Figure 7. Loran-C time of arrival variations after correction for the value of corresponding air temperature